Virology 489 (2016) 44–50

Contents lists available at ScienceDirect

Virology

journal homepage: www.elsevier.com/locate/yviro

HAdV-2-suppressed growth of SV40 T antigen-transformed mouse mammary epithelial cell-induced tumours in SCID mice

Chengjun Wu [a,1,2], Xiaofang Cao [a,1], Di Yu [b], Elisabeth J.M. Huijbers [a,3], Magnus Essand [b], Göran Akusjärvi [a], Staffan Johansson [a], Catharina Svensson [a,*]

[a] Department of Medical Biochemistry and Microbiology, Uppsala University, Sweden
[b] Department of Immunology, Genetics and Pathology, Uppsala University, Sweden

ARTICLE INFO

Article history:
Received 7 July 2015
Returned to author for revisions
30 October 2015
Accepted 4 November 2015
Available online 18 December 2015

Keywords:
Oncolytic adenovirus
Murine cells
Anti-tumour activity
Permissive infection
Viral replication

ABSTRACT

Human adenovirus (HAdV) vectors are promising tools for cancer therapy, but the shortage of efficient animal models for productive HAdV infections has restricted the evaluation of systemic effects to mainly immunodeficient mice. Previously, we reported a highly efficient replication of HAdV-2 in a non-tumorigenic mouse mammary epithelial cell line, NMuMG. Here we show that HAdV-2 gene expression and progeny formation in NMuMG cells transformed with the SV40 T antigen (NMuMG-T cells) were as efficient as in the parental NMuMG cells. Injection of HAdV-2 into tumours established by NMuMG-T in SCID mice caused reduced tumour growth and signs of intratumoural lesions. HAdV-2 replicated within the NMuMG-T-established tumours, but not in interspersed host-derived tissues within the tumours. The specific infection of NMuMG-T-derived tumours was verified by the lack of viral DNA in kidney, lung or spleen although low levels of viral DNA was occasionally found in liver.

Introduction

Virotherapy, where a virus is designed to specifically kill tumour cells but not normal cells presents a promising trajectory for cancer therapy. Numerous studies have shown that different human viruses can suppress the growth of tumour cells (Russell et al., 2012) and among these, human adenoviruses (HAdVs) have emerged as one of the more attractive candidates since they can be grown to high titres, are easy to genetically modify and have the ability to transduce a wide variety of cells, without integrating into the genome. Clinical studies have also given promising results showing that oncolytic HAdVs can be both safe and efficient (Hemminki, 2014). Non-replicating HAdV vectors armed with suicide genes have the drawback of limited access to all cells within a tumour. In contrast, replicating HAdVs (and preferably conditionally restricted replicating HAdVs) have the capacity for sequential multiplication, release and infection of surrounding cells.

HAdVs show strict host specificity and preclinical research on clinically useful replicating HAdV vectors has been hampered by the lack of an experimental animal model system that can efficiently support HAdV infection and replication. Semi-permissive infections in rodents have been achieved, but the efficiency of wild type HAdV replication is modest (Hallden, 2003; Jiang et al., 2014; Thomas et al., 2006), although it can be enhanced by transgenic expression of surface receptors and viral genes (Kang et al., 2014; Young et al., 2012). Thus, the antitumour efficacy of oncolytic HAdV is normally analysed in human xenografts in immunodeficient mice.

We have previously identified a mouse mammary epithelial cell line, NMuMG, that supports HAdV-2 replication to the same level as observed in commonly used and highly permissive human cell lines, like the lung carcinoma cancer cell line A549 (Wu et al., 2013). NMuMG cells form well-structured and contact-inhibited monolayers and are unable to establish tumours in immunodeficient mice (Hynes et al., 1985). In contrast, we show here that SV40 T antigen-transformed NMuMG cells (NMuMG-T) readily formed tumours in SCID mice, and that these tumours were highly permissive to HAdV-2 replication and responded by a significantly reduced tumour growth and signs of cellular destruction.

Results and discussion

Establishment of the SV40 T-antigen-transformed cell line NMuMG-LT

The NMuMG cell line is derived from normal mouse mammary epithelial cells and retains the growth characteristics of non-transformed primary cells. We recently demonstrated that the

* Correspondence to: Department of Medical Biochemistry and Microbiology, BMC, Uppsala University 751 23 Uppsala, Sweden.
E-mail address: cath@imbim.uu.se (C. Svensson).
[1] These authors contributed equally.
[2] Current address: Division of Medical Microbiology, Lund University, Sweden.
[3] Current address: Angiogenesis Laboratory, Department of Medical Oncology, VU University Medical Center, Amsterdam, The Netherlands.

http://dx.doi.org/10.1016/j.virol.2015.11.031
0042-6822/

NMuMG cells in tissue culture exhibit an amazing capacity to support replication by a number of HAdV types (Wu et al., 2013). Since NMuMG cells are essentially non-tumorigenic after transplantation in mice (Hynes et al., 1985) the ability to analyse the oncolytic properties of HAdV required establishment of a tumorigenic NMuMG cell line. For this purpose, NMuMG cells were infected with an SV40 T-expressing retrovirus (Jat et al., 1986) and after G418 selection, the polyclonal NMuMG-T cells were expanded and the expression of the LT protein was analysed by western blotting (Fig. 1A). Additionally, the growth kinetics and cell morphology of NMuMG-T were analysed and compared to the parental NMuMG cell line. SV40 T antigen expression resulted in cells becoming smaller and growing in less organized foci, thus more similar to a transformed phenotype (Fig. 1B). Furthermore, the proliferation rate (Fig. 1C) and saturation density (not shown) of NMuMG-T cells increased dramatically.

To compare the capacity of NMuMG and NMuMG-T to establish tumours, 4×10^6 cells were implanted subcutaneously in the right hind flank of SCID mice. Although implants of the parental NMuMG cells caused a palpable mass after 3–4 weeks, this mass disappeared over time. At the termination of the experiment (day 49) no tumour mass could be recovered from mice implanted with NMuMG cells. In contrast, implanted NMuMG-T cells continued to grow throughout the experiment and at the end of the experiment (day 49), tumour masses with an average size of 150 mm^3 (approximately 0.2 g) were recovered at the site of injection (Fig. 1D). These results agree with previous reports describing that non-tumorigenic NMuMG cells gained the capacity to generate tumours in immunodeficient mice following introduction of an activated H-ras gene or the polyoma middle T antigen, respectively (Hynes et al., 1985; Salomon et al., 1987).

Efficient virus production in HAdV-2-infected NMuMG-T cells

We have previously shown that HAdV-2 infected NMuMG cells are as efficient as human A549 cells in producing infectious viral progeny (Wu et al., 2013). PCR analysis of viral early (E1A) and late (L3) mRNA expression (Fig. 2A), as well as western blot analysis of late viral proteins (Fig. 2B) demonstrated that infection of NMuMG-T cells similarly allowed efficient HAdV-2 replication. To ensure that NMuMG-T cells also supported HAdV-2 virus production, we compared the production of infectious virus particles following infection of NMuMG and NMuMG-T cells (Fig. 2C). Five million cells were infected with 10 FFU per cell (Philipson, 1961) of HAdV-2 and 48 and 60 h post-infection (pi), intracellular virus particles were isolated and titrated using a limited dilution assay. The produced number of infectious virus particles per cell ('burst size') was almost identical in NMuMG and NMuMG-T cells (Fig. 2C). In agreement with our previous results (Wu et al., 2013), the burst size increased 3–4 fold between 48 and at 60 h pi (Fig. 2C). Thus, virus production in NMuMG and NMuMG-T cells is by far the most efficient that has been described in a mouse cell line so far. Varying, but generally quite modest levels of virus replication have been demonstrated in different murine cell lines (Ganly et al., 2000; Hallden, 2003). A recent report describes a murine lung adenocarcionoma that supports replication of the oncolytic human adenovirus AdTAV-255 (Zhang et al., 2014). Since this study did not correlate the replication efficiency of AdTAV to that of wild-type HAdV it is difficult to compare efficiencies. However, from the presented data it appears that the burst size is significantly smaller than what we observe in NMuMG-T cells.

The coxsackie and adenovirus receptor (CAR) is the primary receptor for most HAdVs, including HAdV-2 (Bergelson et al., 1997) and the infection efficiency of tissue culture cells by CAR-dependent HAdV vectors correlates with CAR-expression. In the

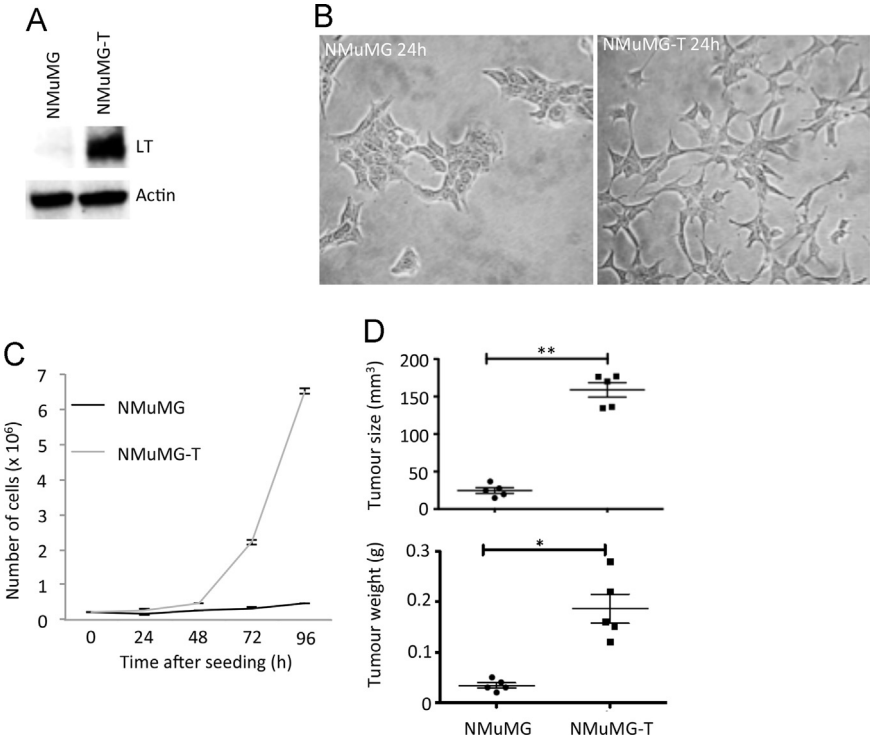

Fig. 1. Growth properties of NMuMG and NMuMG-T. (A) Western blotting analysis of SV40 T antigen expression in NMuMG and NMuMG-T cells. (B) The morphology of sparse cell cultures 24 h after seeding. Note the less extensive cell–cell contacts between NMuMG-T cells compared to NMuMG cells. (C) Proliferation curves of NMuMG and NMuMG-T cells. 200,000 cells were seeded in 35 mm plates. At the indicated time points, cells were collected by trypsin/EDTA treatment and counted. Data represent mean ± standard deviation from triplicate experiments. (D) Comparison of the ability of NMuMG and NMuMG-T cells to establish tumours following subcutaneous implantation. Groups of five SCID mice each were used and tumour volume and weight was determined 49 days after the injection. * and ** represent $P \leq 0.05$ and $P \leq 0.01$ respectively.

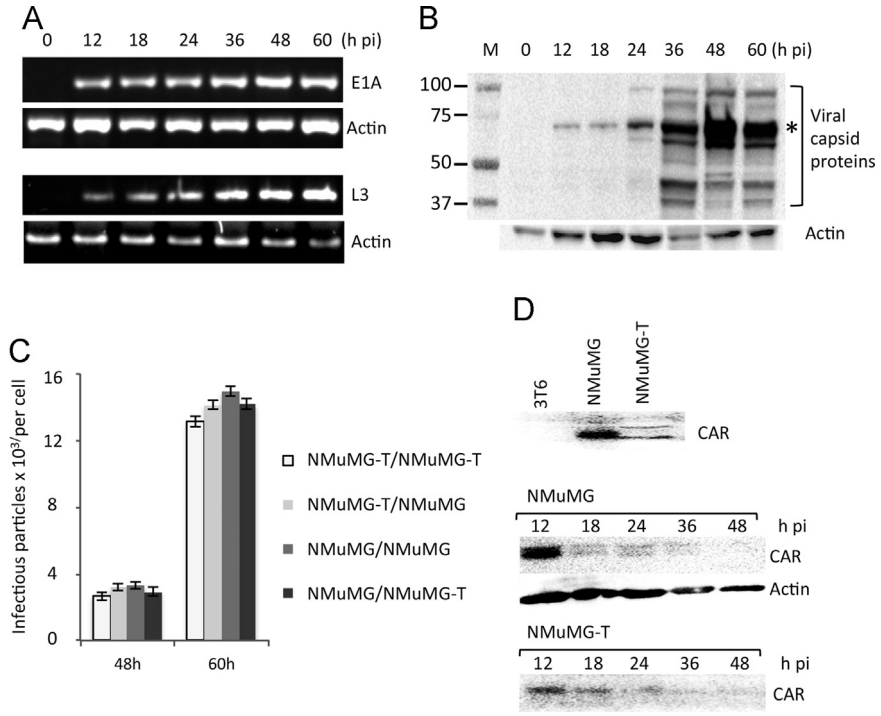

Fig. 2. Efficient replication of HAdV-2 in NMuMG-T cells. (A) RT-PCR analysis of HAdV-2 E1A, L3 and actin mRNA levels in NMuMG-T cells isolated at the indicated time points after HAdV-2 infection. (B) Expression of late viral protein in NMuMG-T cells at the indicated time points after HAdV-2 infection analysed by western blotting using an antibody against HAdV-2 virions (Prage et al., 1970). Note that the polyclonal antibody also detects the non-capsid 72 K protein (*). Actin is shown as an internal control. (C) Production of infectious virus in HAdV-2 infected NMuMG and NMuMG-T cells measured by burst assay. HAdV-2 virus was isolated from infected NMuMG and NMuMG-T cells at 48 h and 60 h pi, and titrated on either NMuMG or NMuMG-T cells. At day six pi, the cytopathic effect was determined and the burst size of the original infection calculated. The pairwise combinations denote the cell line used for the first infection for 48 h or 60 h followed by the cell line used for the titration assay, respectively. (D) The expression of CAR in NMuMG and NMuMG-T cells analysed by western blotting. 3T6 cells were used as a negative control. The gradual decrease in CAR expression in NMuMG or NMuMG-T cells at indicated time points after HAdV-2 infection is shown in the lower part of the figure.

human host, CAR is primarily expressed in tight junctions and on the basolateral membrane and therefore not easily accessible for HAdV upon the first encounter with an epithelium (Philipson and Pettersson, 2004). However, CAR exists in different splice variants, one of which is present on the apical surface of a polarized epithelium and might mediate the initial binding of HAdV (Excoffon et al., 2010). Down-regulation of CAR expression during malignant progression has been demonstrated in different human cancers (Matsumoto et al., 2005). However, up-regulated CAR expression has also been described and the discrepant results might possibly represent alternative regulation of the different splice isoforms (Dietel et al., 2011). Generally, down-regulated CAR expression causes resistance to HAdV oncolytic therapy (Li et al., 1999; Wunder et al., 2012). In agreement with earlier reports (Vincent et al., 2009) our western blot analysis showed that NMuMG cells express CAR (Fig. 2D). Notably, expression of SV40 T in NMuMG-T correlated with a significantly reduced expression of CAR (Fig. 2D). No CAR expression was detected in 3T6 cells serving as a negative control. Surprisingly, the reduced CAR expression level in NMuMG-T cells compared to NMuMG did not impair the ability of HAdV-2 to infect (Fig. 2C), suggesting that CAR was still present in non-limiting amounts on the cell surface or that infection was mediated by alternative receptors. Strikingly, a strong repression of CAR expression was seen upon HAdV-2 infection of both NMuMG and NMuMG-T cells (Fig. 2D). HAdV infection of human cells has been shown to reduce CAR expression in persistently infected lymphocytes, both at the level of reduced cell surface expression and through transcriptional repression (Zhang et al., 2010). While the initial elimination of CAR from the cell surface might depend on its interaction with the adenovirus fiber protein (Zhang et al., 2010), transcriptional silencing of CAR in human cancer cells appears to involve histone deacetylase activity (Wunder et al., 2012). At the moment it is not clear how the observed repression of CAR in NMuMG and NMuMG-T cells occurs, but based on previous reports describing a shift towards transcriptional silencing of host cell genes during the late phase of HAdV infection it may not be unreasonable to assume that the promoter activity of CAR is repressed (Zhao et al., 2007).

HAdV-2 reduces growth of NMuMG-T-induced tumours in SCID mice.

To analyse if HAdV-2 could cause cytolytic replication also in tumours established by NMuMG-T, we performed a pilot experiment where 4×10^6 cells were implanted subcutaneously into the right hind flank of SCID mice. When the tumours had reached an average size of 150 mm^3, the mice were divided into three groups and injected intratumorally with 30 μl PBS (two mice), or PBS containing 10^9 encapsidated viral genomes of UV-inactivated HAdV-2 (two mice) or active HAdV-2 (three mice), respectively. The injections were repeated after seven days and tumour growth was measured every third day until the animals were sacrificed (Fig. 3A). Both HAdV-2 and UV-inactivated HAdV-2 initially reduced tumour growth, but at the end of the experiment, a clear reduction in tumour size was only seen in mice receiving active HAdV-2 (Fig. 3A and B). The initial reduction in tumour growth following injection of UV-inactivated HAdV-2 might indicate that the inactivation step was incomplete. This possibility was supported by the detection of low amounts of viral DNA in mouse blood drawn at day 43 (inset Fig. 3A). Additionally, it is also possible that viral proteins from the UV-inactivated virus exerted a general inhibitory effect on cell proliferation, but that this gradually disappeared as the virus was eliminated. At the end of the experiment no significant difference in tumour size between

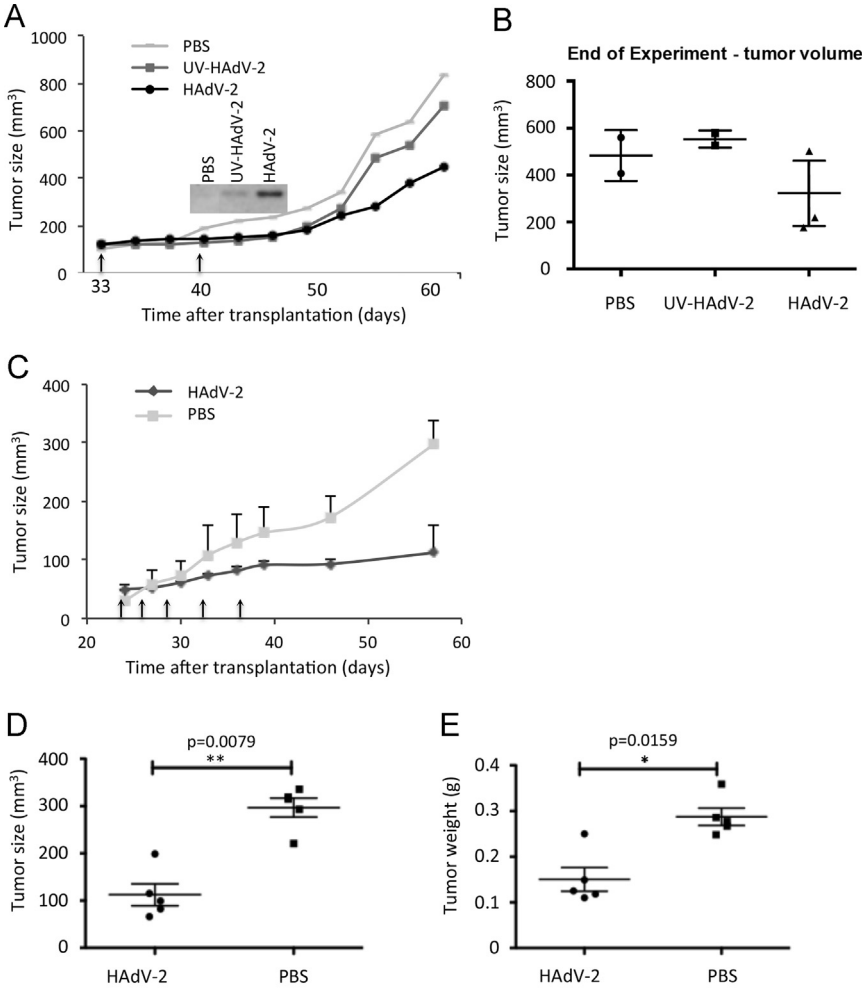

Fig. 3. HAdV-2 inhibits growth of NMuMG-T-established tumour in SCID mice. (A) Initial analysis of the effect of HAdV-2 on NMuMG-T tumour growth. NMuMG-T cells were implanted subcutaneously into the flank of SCID mice. After 33 and 40 days (indicated by arrows) HAdV-2, UV-inactivated HAdV-2, or PBS was injected into the established tumours. Tumour growth was estimated every third day by measuring the size. The data represent mean values of two mice each for the PBS group and the UV-inactivated virus group and three mice for the HAdV-2 injected group. (B) The end volume of the tumours in Fig. 3A. After 61 days the experiment was terminated and the mice were sacrificed. The volume of the excised tumours was determined. (C) Effect of repeated HAdV-2 injections on NMuMG-T tumour growth. HAdV-2 or PBS was injected into NMuMG-T tumours at the time points indicated by the arrows and the size of the tumours was estimated every third day. The data represent mean values ± standard deviation between all mice within each group (six and five mice, respectively). (D and E) The end size of the tumours in Fig. 3C. After 57 days the experiment was terminated and the mice sacrificed. The volume (D) and weight (E) of the excised tumours were determined.

injections with PBS alone and UV-inactivated HAdV-2 was seen (Fig. 3B).

In a second experiment, 12 SCID mice were implanted subcutaneously with the NMuMG-T cells into the right hind flank. Following establishment of the tumours, the mice were divided into two groups that received five injections (on day 21, 24, 27, 33 and 36) with either HAdV-2 or PBS, respectively. Tumour growth was followed by caliper measurement every third day. Mice injected with HAdV-2 exhibited a clear reduction in tumour growth compared to mice treated with PBS alone (Fig. 3C). At day 57 when the experiment was terminated, the tumours were excised, measured and weighed. Except for one outlier, tumours from the HAdV-2-treated mice were significantly smaller in size (Fig. 3D) and weighed less (Fig. 3E) than tumours from PBS-treated mice. It should be noted that, for unknown reasons one mouse treated with HAdV-2 died prematurely.

NMuMG-T-induced tumours support replication of HAdV-2

NMuMG cells are derived from mouse mammary gland epithelium and can thus be identified by immunofluorescent staining using epithelial-specific anti-keratin antibodies. In the absence of a virus infection the tumours established by NMuMG-T cells displayed characteristics of duct/gland structures (Fig. 4A and S1). These tumours were generally well structured and lacked signs of necrosis or disintegrated areas, but showed occasional interspersed regions of non-epithelial (negative for keratin) host stroma cells (arrows in Fig. 4A) and blood vessels (CD31 positive) (Fig. S1). In contrast, the tumours treated with HAdV-2 were less structured and also exhibited areas with disruption of the tumour tissue structures, suggestive of extensive necrosis (Fig. 4B). In tumours injected with HAdV-2, hexon production overlapped with keratin-expressing cells indicating that the virus replicated specifically in NMuMG-T cells. As expected, interspersed non-epithelial host cells in the tumours did not stain for hexon (marked by arrow in Fig. 4B) demonstrating that only NMuMG-T cells were able to support virus replication. This was further illustrated by imaging areas with pronounced infiltration of non-epithelial recipient mouse cells with enhanced signal intensity (Fig. S2) and at higher magnification (Fig. S3). Notably, the intensity of the keratin staining was consistently higher in all the virus-injected tumours than in the PBS-injected tumours, possibly

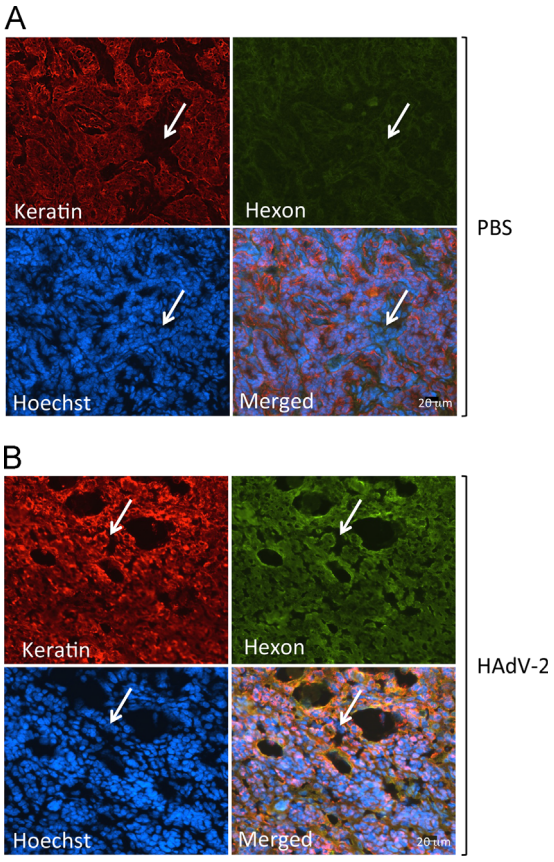

Fig. 4. Immunostaining of tumour sections. Representative images from immunostaining of tumour tissues recovered at day 57 of the experiment described in Fig. 3, panels C–E. (A) NMuMG-T-established tumours injected with PBS. (B) NMuMG-T-established tumours injected with HAdV-2. The sections were immunostained with antibodies against keratin (red) or HAdV hexon protein (green); cell nuclei were counterstained with Hoechst (blue). The arrows mark non-epithelial keratin-negative cells derived from the recipient mice.

reflecting cytopathic effects causing altered antigen exposure (Fig. 4A and B, Fig. S3A and C).

Without expression of a therapeutic transgene it is assumed that an efficient oncolytic capacity of HAdV relies on continuous virus infection, replication, cytolysis and release of produced virus. Immunostaining of excised tumours demonstrated that the HAdV-2 hexon protein was expressed three weeks after the last injection of virus (Fig. 4B, S2 and S3), strongly suggesting an efficient and sustained viral replication. The highly permissive nature of NMuMG-T cells for HAdV infection agrees with the observation that the majority of analysed sections of NMuMG-T-established tumour cells stained positive for hexon expression. In the tumour sections, the localization of hexon appeared to vary from mainly cytoplasmic to throughout the cell (Fig. S2). Although the state of the infected cells in the tumour sections was not addressed beyond determining their origin as NMuMG-T cells, it is possible that the differential localization reflects that some cells were dead or dying, whereas others were still alive but at a late stage of infection.

To verify a sustained replication of HAdV, the excised tumours were used for extraction of viral DNA and proteins. PCR amplification demonstrated that all tumours from mice subjected to intratumoural injection of HAdV-2 contained viral DNA (Fig. 5A). Quantitative PCR analysis showed an extensive viral DNA replication in two of the tumours (between 10^9 and 10^{10} viral genomes/mg tissue), moderate in one and modest in two (Fig. 5B). In agreement with these results, viral structural proteins were easily detectable in the three tumours with the highest amount of viral DNA, whereas lower amounts of viral proteins were observed in the two samples with limited viral DNA replication (Fig. 5C). To our knowledge, sustained HAdV replication following injection of tumours established in mice has not been described before. We find this result interesting since repetitive rounds of viral replication is desirable to obtain extensive HAdV-mediated killing of solid tumours.

PCR analyses failed to demonstrate detectable amounts of viral DNA in lung, spleen or kidney, in any of the animals injected with HAdV-2 (Fig. 5D), suggesting that any systemic distribution of virus from the tumour that may occur did not result in virus replication at these sites. In the two mice showing the strongest intratumoral virus replication (Fig. 5A, mouse 1 and 5), the liver contained detectable amounts of viral DNA (Fig. 5D). However, no late viral proteins could be detected by western blotting in the liver (data not shown) suggesting that viral replication did not occur in livers but that the DNA was more likely taken up by the liver cells from the circulatory system. This is also consistent with the general inability of HAdV to replicate in mice and the apparent lack of viral protein production in the cells surrounding the tumour tissues (Fig. 4B).

In summary, this study demonstrates that a tumorigenic derivative of NMuMG cells can support replication of HAdV-2 when grown as tissue culture cells and, more importantly, also after establishment of tumours in mice. Ongoing replication was observed three weeks after the final injection of HAdV-2. This correlated with a slow tumour growth and signs of disruption of tumour structures. NMuMG cells are derived from the mouse strain Namru (Owens et al., 1974). Despite extensive efforts, we have not been able to retrieve this strain. We do however believe that the combination of NMuMG-T cells and Namru (or a another syngenic mouse strain) would offer an ideal model system for the expanded investigation of the efficacy of oncolytic HAdVs.

Materials and methods

Establishment of NMuMG-T cells

NMuMG cells were infected for 4 h at 37 °C with a recombinant retrovirus that transduce the SV40 T gene along with a neomycin-resistance marker gene (Jat et al., 1986) Transduced cells were obtained after selection with G418 (400 μg/ml). A population of cells with stable expression of SV40 T protein was verified by western blot analysis using an anti-LT antibody (Pallas et al., 1986). The resulting cell line was termed NMuMG-T.

Adenovirus infection

NMuMG and NMuMG-T cells were mock-infected or infected in serum-free DMEM with HAdV-2 at a multiplicity of 10 FFU per cell (Philipson, 1961). After adsorption for one hour at 37 °C in humidified air with 5% CO_2, the medium was replaced with DMEM supplemented with 2% FBS and the infected cells were further incubated at 37 °C in 5% CO_2. At indicated time points cells were harvested by trypsin/EDTA treatment and the cell pellets were snap frozen for further RNA, DNA and/or protein extraction.

Tumour models and virus attack

Five weeks old female SCID mice were housed at the BMC animal facility (Uppsala, Sweden) in individually ventilated cages (two mice per cage). NMuMG-T cells were suspended in ice-cold PBS buffer and 4×10^6 cells in a total volume of 100 μl were implanted subcutaneously in the right hind flank. Mice were treated with intratumoural injections of 30 μl PBS with or without 1×10^9 encapsidated viral genomes of HAdV-2. UV inactivation of

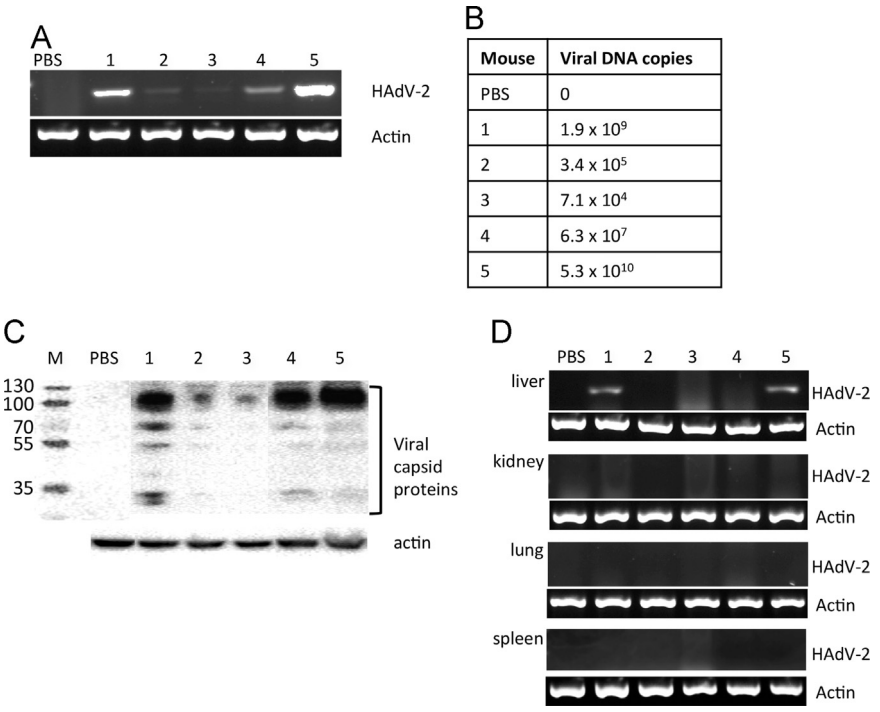

Mouse	Viral DNA copies
PBS	0
1	1.9×10^9
2	3.4×10^5
3	7.1×10^4
4	6.3×10^7
5	5.3×10^{10}

Fig. 5. HAdV-2 replication in NMuMG-T-established tumours. (A) HAdV-2 DNA in NMuMG-T cell tumours analysed by PCR against the E1A gene. DNA from each of the five mice (1–5) described in Fig. 3 panels C–E injected with HAdV-2, as well as one mouse receiving only PBS, was analysed. Actin was used as cellular DNA control. (B) Virus copy numbers (genomes/mg tissue) in the material used in A was quantified by qPCR. (C) Expression of structural viral proteins analysed by western blotting of HAdV-2 structural proteins (Abcam). Samples are as described in A. Actin was used as marker for total protein loading. (D) Presence of HAdV-2 DNA in mouse organs. Viral DNA in different organs was analysed using PCR against the E1A gene. Actin was used as cellular DNA control. The numbers above each lane represent organs from the mice described in A.

HAdV-2 was performed essentially as described in (Stein and Falck-Pedersen, 2012) by irradiating the virus sample at 365 nm for 20 min in the presence of 1 μg/ml of Psoralen (Sigma, Germany). Tumour growth was monitored by caliper measurement and the tumour volume was calculated using the ellipsoid volume formula (length × width × depth × π/6). Blood was collected from the tail vein of the mice and DNA was isolated using QIAamp DNA blood Mini kit (Qiagen). The mice were sacrificed before the tumours reached a size larger than 900 mm^3. Tumour, liver, spleen and lung samples from each mouse were isolated separately. A part of each sample was snap frozen for DNA and protein extraction, and the remaining tissues were fixed in 4% formalin for analysis by immunostaining.

DNA and RNA preparation and PCR analysis

To prepare DNA, collected tissue culture cells were resuspended in lysis buffer (100 mM NaCl, 10 mM Tris–HCl pH 8.0, 25 mM EDTA pH 8.0, 0.5% SDS and 250 μg/ml proteinase K) and treated for 2 h at 37 °C. The samples were centrifuged at 12,000 rpm for 30 min, the supernatants were transferred to new tubes and ethanol-precipitated. The DNA pellets were suspended in TE-buffer. DNA from mouse tissues was isolated using the same method except for addition of a first step where the frozen samples were thawed and grinded in lysis buffer.

PCR amplification of viral DNA was performed in a thermocycler using 100 ng of DNA in a total volume of 25 μl using primers for HAdV-2 E1A 5′-GTGCCAGCGAGTAGA-3′ and 5′-GTCAGAAAACC TGGT-3′, and mouse actin 5′-GGCTGTATTCCCCTCCATCG-3′ and 5′-CCAGTTGGTAACAATGCCATGT-3′. The PCR reaction conditions were: 95 °C 5 min, (95 °C for 20 s, 58 °C for 20 s and 72 °C for 20 s) × 30 cycles, and 72 °C 10 min. The PCR products were analysed by electrophoresis in 1.2% agarose gels.

The QPCR was performed using 50 ng DNA and iQTM SYBR Green Supermix (Bio-Rad) in a Miniopticon Real-Time PCR System (Bio.Rad, CFB-3120) and the E1A primers described above. Cycles conditions were 95 °C 10 min (95 °C for 15 s, 58 °C for 20 s, and 72 °C for 20 s) × 40. All samples were analysed in technical triplicate.

Preparation of mRNA from tissue culture cells, cDNA synthesis and PCR were performed as described before (Wu et al., 2013).

Protein preparation and western blot analysis

Collected cell pellets were lysed on ice for 30 min in RIPA buffer (50 mM Tris–HCl, pH 7.4, 150 mM NaCl, 1% deoxycholate, 1% Tween-20 and protease inhibitors (Roche)). Frozen tumour samples were cut into pieces with a razor blade, grinded in RIPA buffer and lysed on ice for 30 min. Lysates were centrifuged at 12,000 rpm for 10 min at 4 °C, and the supernatants were collected. 15 μg of protein lysate was mixed with 2 × Laemmli sample buffer (62.5 mM Tris–HCl pH 6.8, 25% glycerol, 0.01% BFB and 2% SDS), boiled for 5 min and separated by SDS-PAGE (10%). Following blotting onto an Immobilon-FL Transfer Membrane (Millipore), the membranes were probed with polyclonal antibodies directed against purified HAdV-2 (ab6982, Abcam), (Prage et al., 1970), β-actin (I-19, sc-1616, Santa Cruz), SV40 T-antigen (Pallas et al., 1986), CAR (ad153740, Abcam).

End-point dilution assay

Five million NMuMG-T cells were seeded in 10 cm tissue culture plates and 18 h later infected with HAdV-2 at a multiplicity of 10 FFU/cell (Philipson, 1961). Cell pellets were collected at 48 h and 60 h pi, respectively. The pellets were suspended in 1 ml serum-free medium, freeze-thawed three times and cleared from debris by centrifugation at 10,000*g* in an Eppendorf centrifuge. The supernatants were diluted to 10 ml in serum-free medium and filtered (0.45 μm, Millipore). Each sample was titrated by the limiting dilution method (tissue culture inhibitory dose at 50%:

TCID50) on sub-confluent monolayers of NMuMG or NMuMG-T cells in 96-well plates (10^4 cells/well). Infected plates were incubated at 37 °C in humidified air containing 5% CO_2 for 6 days at which the wells showing a cytopathic effect were determined using a DMRIB inverted microscope (Lecia). Each assay was repeated three times and the virus titres expressed as infectious particles/cell ± SD(Wu et al., 2013)

Immunohistochemistry following HAdV-2 attack on tumours

Cryosections (5 μm) of formalin-fixed tumours were stained with rabbit polyclonal anti-keratin antibody (C2562, Sigma-Aldrich), mouse anti-hexon antibody (MAB8052, Millipore) and anti-CD31 antibody (553370; BD Pharmingen; BD Biosciences). Secondary goat anti-rabbit antibodies conjugated with Alexa Fluor 594 (Life Technologies, 1:1000) or goat anti-mouse conjugated with Alexa Fluor 488 (Life Technologies, 1:400) were used. Nuclei were visualized with Hoechst (H1399, Invitrogen, 1:1000). ProLong Gold anti-fade reagent (1389854, Life Technologies) was used to mount stained sections. Pictures were taken with a Nikon Eclipse 90i microscope, using the 20× or 40× objectives and the NIS Elements 3.2 software with the same exposure time for all samples.

Statistical analysis

Statistical analysis was performed by using GraphPad Prism software version 5.01 (GraphPad software, San Diego, CA). Tumour size in different treatment groups were compared by using two-way analysis of variance.

Biosafety level and ethics declaration

All experiments using HAdV2 were conducted under biosafety level 2 and approved by The Swedish Work Environment Authority. The Uppsala Animal Ethics Committee approved the animal studies (C215/12).

Acknowledgment

This work was supported by grants from the Swedish Cancer Society. The authors express sincere gratitude to Anna-Karin Olsson for support regarding the cell implantation experiments.

The authors declare no conflict of interest.

Appendix A. Supplementary material

Supplementary data associated with this article can be found in the online version at http://dx.doi.org/10.1016/j.virol.2015.11.031.

References

Bergelson, J.M., Cunningham, J.A., Droguett, G., Kurt-Jones, E.A., Krithivas, A., Hong, J.S., Horwitz, M.S., Crowell, R.L., Finberg, R.W., 1997. Isolation of a common receptor for Coxsackie B viruses and adenoviruses 2 and 5. Science 275, 1320–1323.

Dietel, M., Häfner, N., Jansen, L., Dürst, M., Runnebaum, I.B., 2011. Novel splice variant CAR 4/6 of the coxsackie adenovirus receptor is differentially expressed in cervical carcinogenesis. J. Mol. Med. 89, 621–630. http://dx.doi.org/10.1007/s00109-011-0742-6.

Excoffon, K.J.D.A., Gansemer, N.D., Mobily, M.E., Karp, P.H., Parekh, K.R., Zabner, J., 2010. Isoform-specific regulation and localization of the coxsackie and adenovirus receptor in human airway epithelia. PloS One 5, e9909. http://dx.doi.org/10.1371/journal.pone.0009909.

Ganly, I., Mautner, V., Balmain, A., 2000. Productive replication of human adenoviruses in mouse epidermal cells. J. Virol. 74, 2895–2899.

Hallden, G., 2003. Novel immunocompetent murine tumor models for the assessment of replication-competent oncolytic adenovirus efficacy. Mol. Ther. 8, 412–424. http://dx.doi.org/10.1016/S1525-0016(03)00199-0.

Hemminki, A., 2014. Oncolytic immunotherapy: where are we clinically? Scientifica, 1–7. http://dx.doi.org/10.1155/2014/862925.

Hynes, N.E., Jaggi, R., Kozma, S.C., Ball, R., Muellener, D., Wetherall, N.T., Davis, B.W., Groner, B., 1985. New acceptor cell for transfected genomic DNA: oncogene transfer into a mouse mammary epithelial cell line. Mol. Cell. Biol. 5, 268–272.

Jat, P.S., Cepko, C.L., Mulligan, R.C., Sharp, P.A., 1986. Recombinant retroviruses encoding simian virus 40 large T antigen and polyomavirus large and middle T antigens. Mol. Cell. Biol. 6, 1204–1217.

Jiang, H., Clise-Dwyer, K., Ruisaard, K.E., Fan, X., Tian, W., Gumin, J., Lamfers, M.L., Kleijn, A., Lang, F.F., Yung, W.-K.A., Vence, L.M., Gomez-Manzano, C., Fueyo, J., 2014. Delta-24-RGD oncolytic adenovirus elicits anti-glioma immunity in an immunocompetent mouse model. PloS One 9, e97407. http://dx.doi.org/10.1371/journal.pone.0097407.

Kang, S., Kim, J.-H., Kim, S.Y., Kang, D., Je, S., Song, J.J., 2014. Establishment of a mouse melanoma model system for the efficient infection and replication of human adenovirus type 5-based oncolytic virus. Biochem. Biophys. Res. Commun., 1–6. http://dx.doi.org/10.1016/j.bbrc.2014.09.107.

Li, Y., Pong, R.C., Bergelson, J.M., Hall, M.C., Sagalowsky, A.I., Tseng, C.P., Wang, Z., Hsieh, J.T., 1999. Loss of adenoviral receptor expression in human bladder cancer cells: a potential impact on the efficacy of gene therapy. Cancer Res. 59, 325–330.

Matsumoto, K., Shariat, S.F., Ayala, G.E., Rauen, K.A., Lerner, S.P., 2005. Loss of coxsackie and adenovirus receptor expression is associated with features of aggressive bladder cancer. Urology 66, 441–446. http://dx.doi.org/10.1016/j.urology.2005.02.033.

Owens, R.B., Smith, H.S., Hackett, A.J., 1974. Epithelial cell cultures from normal glandular tissue of mice. J. Natl. Cancer Inst. 53, 261–269.

Pallas, D.C., Schley, C., Mahoney, M., Harlow, E., Schaffhausen, B.S., Roberts, T.M., 1986. Polyomavirus small t antigen: overproduction in bacteria, purification, and utilization for monoclonal and polyclonal antibody production. J. Virol. 60, 1075–1084.

Philipson, L., 1961. Adenovirus assay by the fluorescent cell-counting procedure. Virology 15, 263–268.

Philipson, L., Pettersson, R.F., 2004. The coxsackie-adenovirus receptor – a new receptor in the immunoglobulin family involved in cell adhesion. Curr. Top. Microbiol. Immunol. 273, 87–111.

Prage, L., Pettersson, U., Hoglund, S., Lonberg-Holm, K., Philipson, L., 1970. Structural proteins of adenoviruses. IV. Sequential degradation of the adenovirus type 2 virion. Virology 42, 341–358.

Russell, S.J., Peng, K.-W., Bell, J.C., 2012. Oncolytic virotherapy. Nat. Biotechnol. 30, 658–670. http://dx.doi.org/10.1038/nbt.2287.

Salomon, D.S., Perroteau, I., Kidwell, W.R., Tam, J., Derynck, R., 1987. Loss of growth responsiveness to epidermal growth factor and enhanced production of alpha-transforming growth factors in ras-transformed mouse mammary epithelial cells. J. Cell. Physiol. 130, 397–409. http://dx.doi.org/10.1002/jcp.1041300313.

Stein, S.C., Falck-Pedersen, E., 2012. Sensing adenovirus infection: activation of interferon regulatory factor 3 in RAW 264.7 cells. J. Virol. 86, 4527–4537. http://dx.doi.org/10.1128/JVI.07071-11.

Thomas, M.A., Spencer, J.F., La Regina, M.C., Dhar, D., Tollefson, A.E., Toth, K., Wold, W.S.M., 2006. Syrian hamster as a permissive immunocompetent animal model for the study of oncolytic adenovirus vectors. Cancer Res. 66, 1270–1276. http://dx.doi.org/10.1158/0008-5472.CAN-05-3497.

Vincent, T., Neve, E.P.A., Johnson, J.R., Kukalev, A., Rojo, F., Albanell, J., Pietras, K., Virtanen, I., Philipson, L., Leopold, P.L., Crystal, R.G., de Herreros, A.G., Moustakas, A., Pettersson, R.F., Fuxe, J., 2009. A SNAIL1–SMAD3/4 transcriptional repressor complex promotes TGF-β mediated epithelial–mesenchymal transition. Nat. Cell Biol. 11, 943–950. http://dx.doi.org/10.1038/ncb1905.

Wu, C., Öberg, D., Rashid, A., Gupta, R., Mignardi, M., Johansson, S., Akusjärvi, G., 2013. A mouse mammary epithelial cell line permissive for highly efficient human adenovirus growth. Virology 435, 363–371. http://dx.doi.org/10.1016/j.virol.2012.10.034.

Wunder, T., Schmid, K., Wicklein, D., Groitl, P., Dobner, T., Lange, T., Anders, M., Schumacher, U., 2012. Expression of the coxsackie adenovirus receptor in neuroendocrine lung cancers and its implications for oncolytic adenoviral infection. Cancer Gene Ther. 20, 25–32. http://dx.doi.org/10.1038/cgt.2012.80.

Young, A.-M., Archibald, K.M., Tookman, L.A., Pool, A., Dudek, K., Jones, C., Williams, S.L., Pirlo, K.J., Willis, A.E., Lockley, M., McNeish, I.A., 2012. Failure of translation of human adenovirus mRNA in murine cancer cells can be partially overcome by L4-100K expression in vitro and in vivo. Mol. Ther. 20, 1676–1688. http://dx.doi.org/10.1038/mt.2012.116.

Zhang, L., Hedjran, F., Larson, C., Perez, G.L., Reid, T., 2014. A novel immunocompetent murine model for replicating oncolytic adenoviral therapy. Cancer Gene Ther. 22, 17–22. http://dx.doi.org/10.1038/cgt.2014.64.

Zhang, Y., Huang, W., Ornelles, D.A., Gooding, L.R., 2010. Modeling adenovirus latency in human lymphocyte cell lines. J. Virol. 84, 8799–8810. http://dx.doi.org/10.1128/JVI.00562-10.

Zhao, H., Granberg, F., Pettersson, U., 2007. How adenovirus strives to control cellular gene expression. Virology 363, 357–375. http://dx.doi.org/10.1016/j.virol.2007.02.013.